2018

Mechanical Wear Debris Feature, Detection, and Diagnosis: A Review

Wei Hong

Wenjian Cai

Shaoping Wang

Mileta M. Tomovic
Old Dominion University, mtomovic@odu.edu

Original Publication Citation

Hong, W., Cai, W. J., Wang, S. P., & Tomovic, M. M. (2018). Mechanical wear debris feature, detection, and diagnosis: A review. *Chinese Journal of Aeronautics, 31*(5), 867-882. doi:10.1016/j.cja.2017.11.016

Chinese Journal of Aeronautics, (2018), 31(5): 867–882

Chinese Society of Aeronautics and Astronautics
& Beihang University

Chinese Journal of Aeronautics

cja@buaa.edu.cn
www.sciencedirect.com

Mechanical wear debris feature, detection, and diagnosis: A review

Wei HONG [a], Wenjian CAI [a], Shaoping WANG [b,c,*], Mileta M. TOMOVIC [d]

[a] School of Electrical and Electronic Engineering, Nanyang Technological University, 639798, Singapore
[b] School of Automation Science and Electric Engineering, Beihang University, Beijing 100083, China
[c] Science and Technology on Aircraft Control Laboratory, Beijing 100083, China
[d] Mechanical and Aerospace Engineering Department, Old Dominion University, VA 23529, USA

Received 26 March 2017; revised 1 June 2017; accepted 18 July 2017
Available online 5 December 2017

KEYWORDS

Debris detection;
Debris feature;
Fault diagnosis;
Mechanical wear debris;
Wear mechanism

Abstract Mechanical debris is an important product of friction wear, which is also a crucial approach to know the running status of a machine. Many studies have been conducted on mechanical debris in related fields such as tribology, instrument, and diagnosis. This paper presents a comprehensive review of these studies, which summarizes wear mechanisms (e.g., abrasive wear, fatigue wear, and adhesive wear) and debris features (e.g., concentration (number), size, morphology, and composition), analyzes detection methods principles (e.g., offline: spectrograph and ferrograph, and online: optical method, inductive method, resistive-capacitive method, and acoustic method), reviews developments of online inductive methods, and investigates the progress of debris-based diagnosis. Finally, several notable problems are discussed for further studies.

1. Introduction

In a running machine, failure is unavoidable if maintenance is not conducted in time. For crucial or expensive machines, breakdown maintenance could not be allowed because of high safety risk or economic loss, while time-based preventive maintenance may cost much more than the scheme using different strategies to machines in different health conditions.[1] Therefore, an effective way to have both high reliability and low cost is to perform condition-based maintenance through offline or online detection.

To identify machine health condition, the failure mechanism should be known. Among failure modes, wear fault is the most common type which is unavoidable. Although different friction pairs exist in a machine, they are essentially composed of two friction surfaces which move with respect to each other. Their functions are transferring and transforming power so that the machine could achieve a specified movement. During the movement, power is inevitably lost in the movement, which is dissipated as heat and vibration and damages friction surfaces.[2] By ignoring the running-in period, the wear

* Corresponding author at: School of Automation Science and Electric Engineering, Beihang University, Beijing 100083, China.
E-mail address: shaopingwang@vip.sina.com (S. WANG).

Peer review under responsibility of Editorial Committee of CJA.

Production and hosting by Elsevier

https://doi.org/10.1016/j.cja.2017.11.016
1000-9361 © 2017 Chinese Society of Aeronautics and Astronautics. Production and hosting by Elsevier Ltd.

rate of a friction pair is almost continuously increasing.[3] In the early stage of this wear process, the friction surface gradually becomes rough caused by debris generation that will increase the mechanical vibration. The friction surface is also heated by the energy released from asperity deformation so the metal performance of the wear surface would be further degraded. These two effects lead to that friction wear becomes more and more severe and finally causes component damage and system failure.

Many centuries ago, people already knew that wear debris is generated with a wear process.[4] Especially, it was found nearly a century ago that wear debris is strongly related to the condition of friction.[5] Compared to the other two visible indicators, temperature and vibration, using wear debris as an indicator for machine health has some distinguished advantages such as strong relationship to wear surface profile, long persistence of information, and strong anti-interference capacity. Due to these reasons, using wear debris to investigate the health conditions of machines has attracted much attention since 1950s.[6] Many detection methods have been developed in the past few decades that debris information becomes an important indicator for mechanical health status.[7] Currently, online debris monitoring has been applied in commercial engines,[8] fighters' engines,[9] helicopters' gearboxes,[10] and wind turbines[11] to increase system reliability and reduce maintenance cost.

As many factors such as wear mechanism, debris feature, detection method, and signal processing and diagnosis technique affect the accuracy and reliability of debris-based diagnosis, it is, therefore, beneficiary to have an overall review on the research progresses and discuss the key problems and solutions. In this paper, we will provide an overview on these issues and summarize their connections. The remaining sections of this paper are organized as follows. In Section 2, different wear mechanisms for debris generation are investigated. Section 3 summarizes the relationship between debris features and wear types. Section 4 introduces the principles of debris detection. The developments of online inductive methods and signal processing are reviewed in Section 5. Section 6 presents the research progresses of debris-based diagnosis. Finally, some notable problems are discussed in Section 7.

2. Wear mechanisms

In a friction pair, the wear mechanism depends on the load, sliding speed, hardness and roughness of the wear surface, lubrication, and so on; meanwhile, the debris feature and wear type are two external manifestations of the wear mechanism.[3] Therefore, the wear mechanism is a key bond to link the debris feature and wear type. To consider the reasons for debris generation, the wear mechanism can be classified into three types: abrasive wear, fatigue wear, and adhesive wear,[12] as shown in Fig. 1.

Abrasive wear usually occurs between soft surfaces and hard asperities. In this wear type, an asperity is striped and becomes a debris particle when the asperity is not strong enough, which generally happens in the running-in period, and the debris usually is tiny. Otherwise, the asperity may make scratches on the soft surface and produce a cutting debris when the asperity is solid, and the debris is usually elongated. An early study[13] indicated that the debris volume is

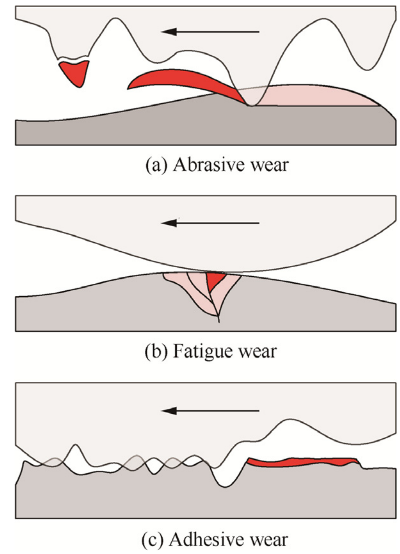

Fig. 1 Three wear mechanisms.

proportional to the load and sliding distance. Further studies[14–16] used the Archard equation to describe the wear rate shown in Eq. (1). In a stable wear condition, the value of K is constant. The typical value is in the range of 0.005–0.05 in two-body wear and tends to be lower than 0.0005 in three-body wear.[3] However, a complete wear test under a nominally constant condition indicated that the wear rate is variable: the initial and final stages are high and the middle stage is stably low, as shown in Fig. 2, which is one of the reasons why the mechanical failure rate is a Bath Curve.

$$W = K\frac{PV}{H} \tag{1}$$

where W is the wear rate, K is the wear coefficient, P is the load on the friction pair, V is the sliding speed, and H is the hardness of the wear surface.

Fatigue wear generally occurs on periodical contact surfaces such as those of bearings and gears. As a periodical force makes a material fatigue, the wear surface would be broken into many irregularly blocky debris particles and similar to pitting even grooves. In this case, the wear rate is not too high, but the vibration will be rapidly increased when pitting is formed. Therefore, this wear type may easily cause system failure. Studies of rolling fatigue[17–19] indicted that the fatigue initiation is in 10%–40% of useful life. Furthermore, Leng et al.[19] studied growth of fatigue cracks, and found that subsurface cracks tend to initiate at non-metallic inclusions and their

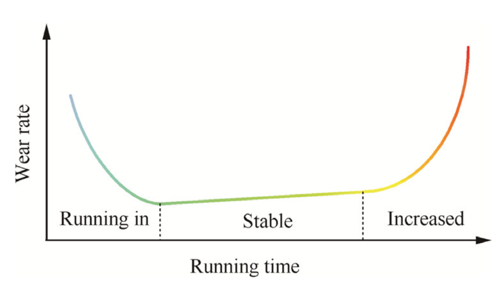

Fig. 2 Change of the wear rate.

directions are 20°–30° to the direction of the contact motion. Finally, a lot of debris particles will be generated when the cracks extend to the surface. As friction surfaces in a gear are insufficiently smooth and clear, asperities will raise local stresses and cause surface pits.[20,21] These pits are 5–25 μm deep and exist on most of the contact area; as a result, a large number of tiny debris particles are generated in this case.[22] By contrast, friction surfaces in a bearing are so smooth that the oil film could separate motion surfaces, which is why the fatigue damage of a bearing is quite different from a gear's pitting. The fatigue form of early bearings is subsurface crack because of material quality, but now the fatigue form usually is surface damage caused by debris in lubricant.[23,24] Different from a stable increase in a gear, debris generation in a bearing suddenly increases when a macro damage is formed.[25]

Adhesive wear is a dangerous type, in which a lot of asperities bite each other, and the temperature on the friction surface quickly increases so that wear conditions such as material property, and lubrication would further deteriorate.[26] A four-ball test[27,28] indicated that metal transfer obviously happens in adhesive wear, which means that pieces of metal are peeled from the friction surface during the wear, and the debris generally is flat. The rate of adhesive wear also follows the Archard equation, but the wear coefficient K is in the range of 5×10^{-3}–5×10^{-7}. In order to build a model of the wear coefficient, Rabinowicz[29] analyzed the fracture forms of adhesive junction in a micro scale and described their probabilities based on the stress-strength interference theory to obtain the wear coefficient in a macro scale. Blau[30] studied temperature effects on adhesive wear in dry sliding contacts, and experimental results indicated that a vicious circle exists between surface temperature and friction wear. Although the rate of adhesive wear is not too high, the component is easy to break down suddenly because of increasing friction caused by adhesion. Therefore, adhesive wear is an omen of component fault.

Table 1 Relationship between wear features and debris features.

Debris feature	Wear feature			
	Severity	Rate	Type	Location
Concentration	×	×		
Size	×	×	×	
Morphology	×		×	×
Composition				×

Note: × means related.

3. Debris features

Through many studies,[31–36] engineers found that different wear behaviors apparently show up in four debris features: concentration (number), size, morphology, and composition, as shown in Table 1. Since debris concentration and size both increase by increasing of wear degree, they can reflect wear severity and wear rate.[31] Meanwhile, debris size can also indicate wear types.[34] On the other hand, wear severity and type depend on wear condition which also determines debris morphology, so debris morphology is related to wear severity and type even location.[35] In addition, different materials are applied to specified friction pairs to optimize the useful life for different working conditions[36]; therefore, wear location could be estimated through debris composition.

Based on some instruments such as particle counters and ferrograph, debris concentration and size can be obtained to demonstrate the wear process.[7] However, the processes of each component are variable because of differences in individuals and loads; therefore, it is less confident to specify some precise thresholds to divide wear stages. In order to distinguish different wear statuses, Bowen and Anderson systemically studied the relationship between debris size and wear type.[34,37] They analyzed debris generated from five typical wear types:

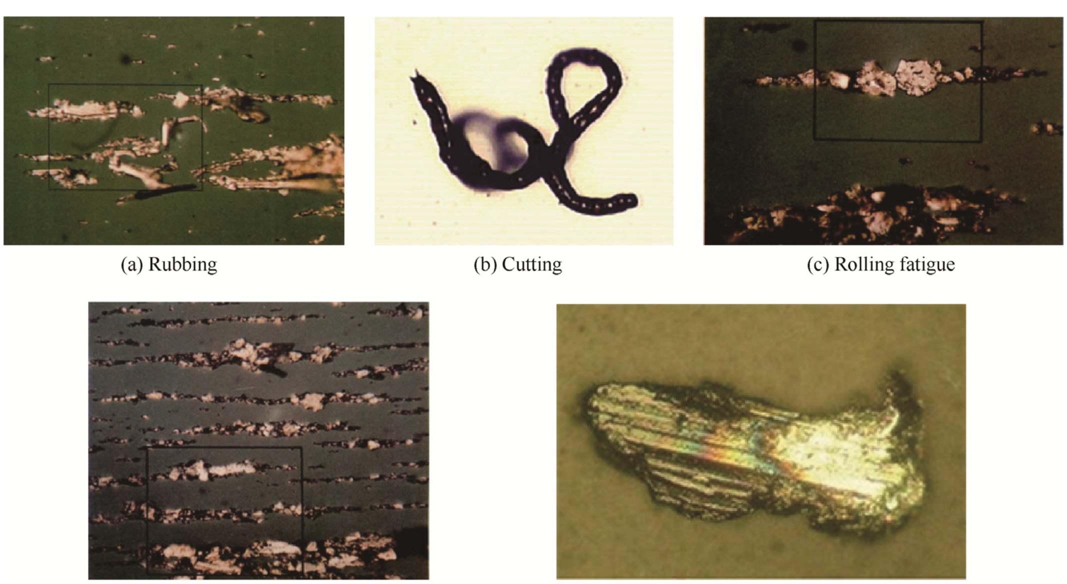

(a) Rubbing (b) Cutting (c) Rolling fatigue (d) Combined rolling and sliding (e) Sliding and severe sliding

Fig. 3 Five typical debris types.[38]

rubbing, cutting, rolling fatigue, combined rolling and sliding, and severe sliding, as shown in Fig. 3.

The debris features of these five wear types are shown in Table 2. Rubbing debris comes from normal sliding wear, as shown in Fig. 3(a). Its equal diameter is 0.5–15 μm, thickness is 0.15–1 μm, and diameter-to-thickness ratio is from 3:1 to 10:1. Cutting debris is from soft friction surface and dug by a hard asperity, as shown in Fig. 3(b). The debris is spindly, of which the width is 2–5 μm and the length is 25–100 μm. Rolling fatigue wear is caused by periodical rolling contact (e.g., bearings), where the debris is blocky and flat as shown in Fig. 3(c). The equal diameter is 10–100 μm and the ratio between the diameter and thickness is about 10:1. Combined rolling and sliding wear usually occurs on gear surface, and the diameter-to-thickness ratio of debris is from 4:1 to 10:1 depending on the involute profile of the gear, as shown in Fig. 3(d). In this wear type, big debris has a higher percentage than that of small debris. Severe sliding usually happens in a friction pair with a high load and a low speed, in which debris is bigger than 15 μm and the diameter-to-thickness ratio is about 10:1. In addition, striations and straight edges are apparent marks in this debris morphology, and the ratio of large-to-small debris is related to the limit exceeding of surface stress. This study indicated that debris size could roughly distinguish wear types, and especially, debris above 15 μm is from abnormal wear.

Roylance and Pocock[39,40] analyzed actual debris in the range of 1–20 μm based on Ferrograph, and they found that the Weibull function is suitable to describe the distribution between debris size and number so that distribution parameters can reflect the wear progress. However, in further studies, Dempsey et al.[25] monitored operations of gears and bearings by using a MetalSCAN sensor which can online detect oil debris above 125 μm, and they considered that debris distribution in the sensitivity range is difficult to distinguish component statuses between normal and fault. This conclusion conflicts with the studies of Roylance and Pocock,[39,40] which is probably caused by different detection ranges, but it also indicated that severe wear at the micro level is prior to apparent damage at the macro level.

Since debris morphology is closely related to wear type and has abundant attributes, engineers have studied it through optical microscopy and scanning electron microscopy, and they considered that a good way to inspect a wear process is to classify wear mechanisms or types through attributes.[41] Among these attributes, debris thickness[42,43] and color[44,45] are two obvious ones, but they are not commonly used because of low cost-effectiveness in their extractions. Conversely, aspect ratio[46] and roundness factor[35] are more popular. Since the range of debris sizes overlaps between different debris types, more details of debris outlines need to be utilized for further classification. A sample indicator is the angle defined

Table 2 Debris features of five typical wear types.

Wear type	Debris feature			
	Equal diameter (μm)	Thickness (μm)	Ratio	Morphology
Rubbing	0.5–15	0.15–1	3:1–10:1	Tiny
Cutting	25–100 (length)	2–5 (width)	12:1–20:1	Spindly
Rolling fatigue (bearing)	10–100	1–10	10:1	Blocky and flat
Combined rolling and sliding (gear)			4:1–10:1	Irregular
Severe sliding	> 15		10:1	Striations and straight edges

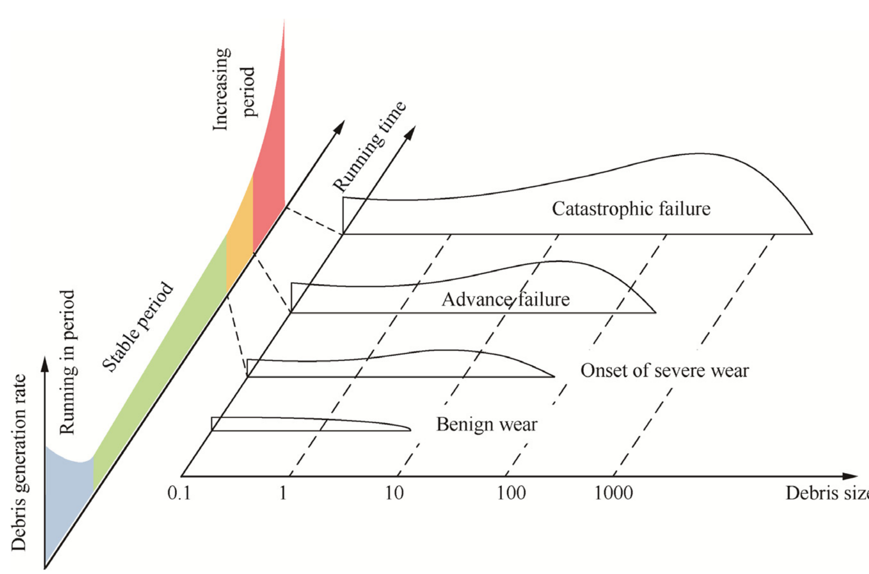

Fig. 4 Relationship between debris generation and wear process.[69]

by three specified points on a debris outline.[47] Moreover, a set of outline sequences is defined as radius differences from the equal circle so that some analytical methods such as Fourier transform can be easily applied in a sequence.[41,48,49] Based on the fractal theory, a fractal dimension is obtained through measuring the perimeter of a debris outline with different step sizes, which is used to represent the outline feature.[50–58] In addition, surface texture is also an important morphological attribute,[59–63] so debris pictures are processed by grey level analysis,[64] 2D fast Fourier transform,[65] fractal dimension,[66] and pattern recognition.[67]

Through these valuable studies, the relationships between wear type, wear mechanism, and debris feature are roughly known.[68] Among them, Bhushan[69] summarized the relationship between debris generation and wear process as shown in Fig. 4, which has practical guiding significance. However, because of complicated relationships between these three objects and potential differences on individuals, debris classification could only qualitatively determine wear type and mechanism. Therefore, how to quantify a wear process is still a significant challenge.

4. Detection principles

Throughout debris detection techniques, the development is divided into three stages: offline weighting, offline detection based on instruments, and online monitoring based on sensors. In 1950s, engineers regularly collected debris from an oil filter and then weighted the debris mass to know wear severity.[15] As weighting can only get a little information, specific instruments such as spectrograph and ferrograph have been developed since 1960s. Spectrograph uses the light of debris burning to identify debris compositions and contents.[70] In order to simplify this instrument, X-ray fluorescence spectrograph was presented, which uses the light excited from debris and is more convenient than the original spectrograph.[71–73] Ferrograph utilizes a gradient magnetic field to orderly deposit debris particles according to their sizes, and then the distribution and morphology of debris particles can be measured.[7] Although advanced spectrograph and ferrograph have several advantages such as rich information, quick respond, and high accuracy, they are usually offline because of complicated structures, so the wear state may not be provided in real time. Consequently, engineers began to study online debris detection since 1980s and expected to timely obtain the wear state without shutting down a machine.[8,74] As online debris monitoring is a good way to ensure reliable running and achieve condition-based maintenance, it becomes a hotspot in mechanical fault diagnosis.[75]

According to measurement principles, online debris detection can be classified into four types: optical, inductive, resistive-capacitive, and acoustic methods.

The optical method[76–79] includes a pair of light transmitter and receiver, in which light passes through oil flow as shown in Fig. 5. As the light could be blocked by a debris particle, the change of light intensity may reflect the size of the debris particle. This is the most sensitive method at present, which could detect above 5-μm debris in a channel of 1.2 mm by 1.6 mm, but oil transparency and bubbles may seriously affect its result. In addition, such a small channel will cause heavy throttling, so this method is not suitable for big flow conditions, e.g., above 1 L/min.

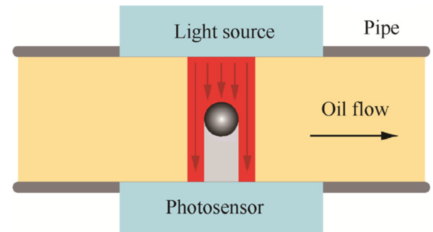

Fig. 5 Schematic diagram of the optical method.

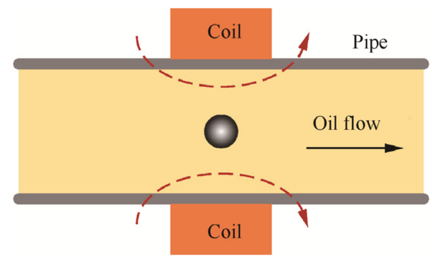

Fig. 6 Schematic diagram of the inductive method.

The inductive method[8,9,74,80–89] is based on electromagnetic induction, in which debris particles will cause a corresponding inductive voltage and an inductance change in inductive coils when the particles go through the sensor, as shown in Fig. 6. In this method, the inductive voltage and inductance change are in proportion to the debris size, and different materials such as ferromagnetic and diamagnetic ones will cause different signature phases. Consequently, the inductive method can provide information about debris sizes and materials. Overall, the advantages of this method are: (a) high throughput, (b) roughly distinguishing debris materials, (c) insensitive to oil quality, and (d) suitable for metal pipes. However, as a magnetic field is passive so that the field is difficult to be concentrated in a specified zone, the sensitivity of the inductive method is relatively poor as detecting 100 μm debris in a pipe with a 12 mm diameter.[9]

In the resistive-capacitive method, a pair of poles is placed on both sides of oil flow as shown in Fig. 7. The electrical field will be disturbed when debris particles pass through the sensor, so debris particles can be detected by measuring resistance[90,91] or capacitance[92–95] between the two poles. By contrast to a magnetic field, an electrical field is active so that the field can be easily limited in a small zone to improve the sensitivity, and thus this method can detect 10-μm debris in a channel with a 40 μm height by a 100 μm width.[94] Because of different permittivity, this method is sensitive to water rather than bubble. Although the sensor structure is very simple, this method is not

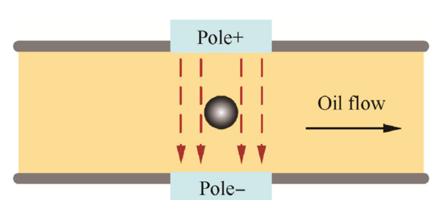

Fig. 7 Schematic diagram of the resistive-capacitive method.

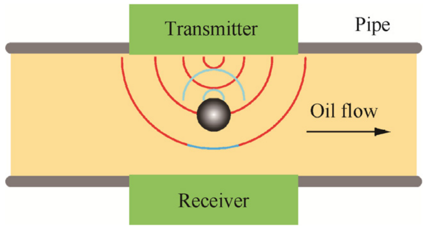

Fig. 8 Schematic diagram of the acoustic method.

Table 3 Comparison of four detection methods.

Method	Detection accuracy	Advantage	Disadvantage
Optical	5 μm in channel of 1.2 mm × 1.6 mm	High sensitivity, morphological information	Affected by bubble and oil transparency, low throughput
Inductive	100 μm in channel of 12 mm diameter	High throughput, distinguish ferromagnetic and diamagnetic, insensitive to oil quality, suitable for metal pipe	Low sensitivity
Resistive-capacitive	10 μm in channel of 40 μm × 100 μm	Simple structure, high sensitivity	Affected by water and oil transparency, cause oil deterioration
Acoustic	75 μm in channel of 6.5 mm × 6.5 mm	Distinguish bubble and solid debris	Affected by oil viscosity, flow speed and mechanical vibration

widely applied because the electrical field would accelerate oil deterioration and oil quality may affect the detection result.

The acoustic method[84,92,96,97] is composed of an acoustic transmitter and an acoustic receiver, which are placed in oil so that acoustic wave can penetrate through oil flow, as shown in Fig. 8. A debris particle would distort a part of transmitted waves and generate some reflex waves when the particle moves into the sensor. Therefore, the strengths of both transmitted waves and reflex waves could reflect the debris size. Based on this method, 75 μm debris could be detected in a channel of 6.5 mm by 6.5 mm, and bubbles could be distinguished from solid debris by the phase of a received wave.[84] However, this method is difficult to be applied in real systems because oil viscosity, flow speed, and mechanical vibration all may affect its performance.

A comparison of these four methods is shown in Table 3.

5. Online inductive method

As unique advantages such as high throughput, distinguishing debris materials, insensitive to oil quality, and suitable for metal pipes would greatly benefit online debris monitoring, engineers have paid more attention to the online inductive method in past thirty years. As early as 1988, Centers and Price[8] monitored the bearing of a GE90 engine through a Quantitative Debris Monitor (QDM) shown in Fig. 9, which could separate air and debris from oil flow and detect above 250-μm debris. The study showed a significant value of online

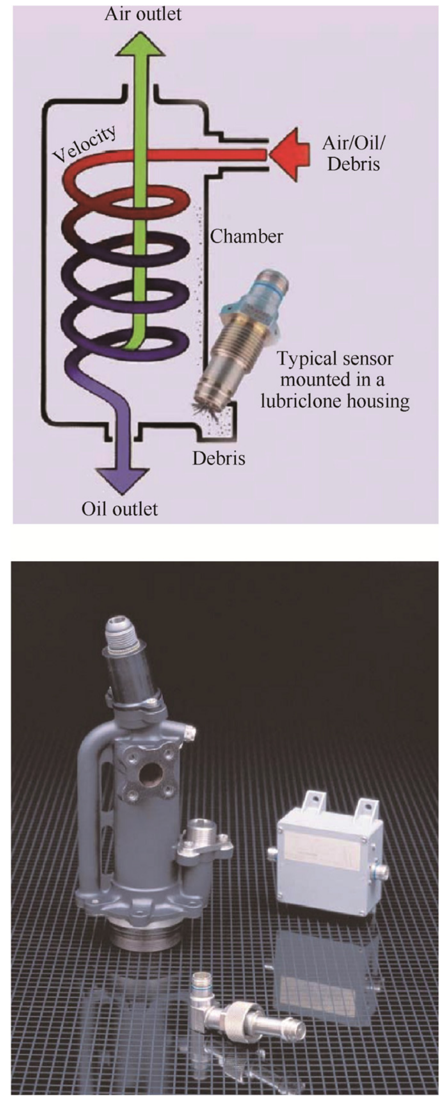

Fig. 9 Quantitative debris monitor.[8]

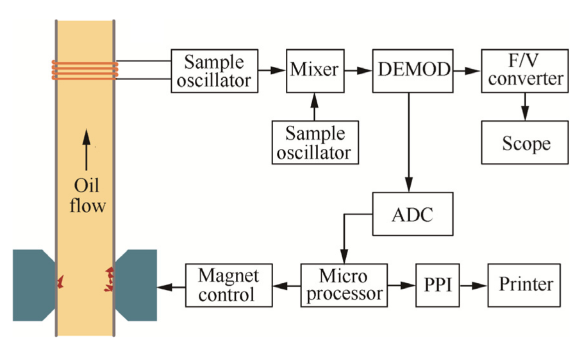

Fig. 10 Debris sensor with electromagnetic collection.[74]

debris monitoring, but the insufficient sensitivity of this sensor was also exposed. At the same period, Chambers et al.[74] designed an inductive sensor with an electromagnet for debris collection, as shown in Fig. 10 (DEMOD: demodulator, ADC: analog to digital converter, F/V Converter: frequency to voltage converter, and PPI: processor peripheral interface). The electromagnet can collect many small debris particles during a period and release them together so that the undetectably small particles could be detected as a big particle. However, the collected proportion is variable depending on magnetic saturation and debris concentration so that a detection result may not truly reflect debris generation. In 1990, Flanagan et al.[80] presented an evaluation method for debris materials based on different changes in an inductive coil's resistance and inductance as shown in Fig. 11 (V_{FM0}: voltage of frequency modulation and V_{AM0}: voltage of amplitude modulation). Moreover, they validated that the method could detect 100 µm ferrous and 200 µm non-ferrous debris within a pipe with a diameter of 6 mm. In the following studies, Gas Tops, a Canadian company, developed a triple-coils sensor called MetalSCAN shown in Fig. 12 (AC: alternating current), in which an inductive coil is placed between two driven coils so that the magnetic field in the inductive coil would be counteracted by the opposite driven fields. Therefore, an inductive voltage will be generated when debris particles pass through the sensor and disturb the balance. In addition, this sensor can distinguish ferromagnetic and diamagnetic debris through the phase of debris signature. The experiment verified that the sensor could detect above 125 µm ferrous debris within a pipe with a diameter of 1/2 inch.[9]

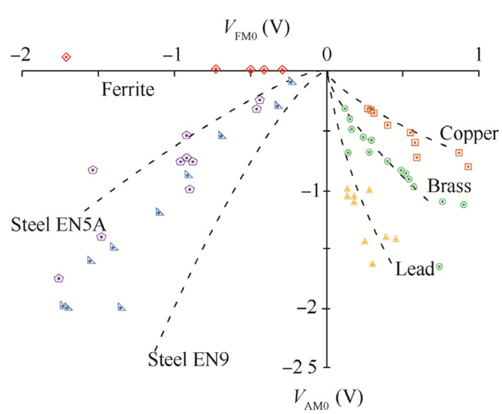

Fig. 11 An evaluation method for debris materials.[80]

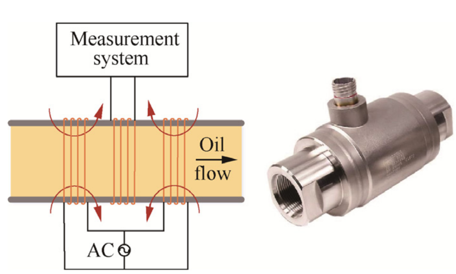

Fig. 12 Schematic diagram of debris sensor MetalSCAN.

However, the related studies[3,68,77] indicated that the debris size is between 1 and 20 µm in normal wear and between 50 and 100 µm in abnormal wear. Especially, debris particles above 200 µm are probably generated in the late stage of the mechanical useful life.[8] In order to increase confidence for diagnosis results and schedule maintenance leisurely, the sensitivity of the inductive method should be improved. For this goal, Du et al.[81,82] analyzed the magnetic field generated by a coil with different ratios of length to diameter, and they proposed that a low length-to-diameter ratio could benefit sensitivity, so they presented two sensor structures shown in Fig. 13 (LCR Meter: inductance-capacitance resistance meter, PDMS: polydimethylsiloxane, H: height of the flow channel, and L: length of the flow channel). The experiment indicated that their sensors could detect above 50 µm debris within a channel with a 250 µm height by a 500-µm width or a pipe with a diameter of 1.2 mm. Soon later, they used the LC resonance method to improve sensitivity as shown in Fig. 14 (C_p: capacitance) so that 20-µm ferromagnetic debris and 55 µm diamag-

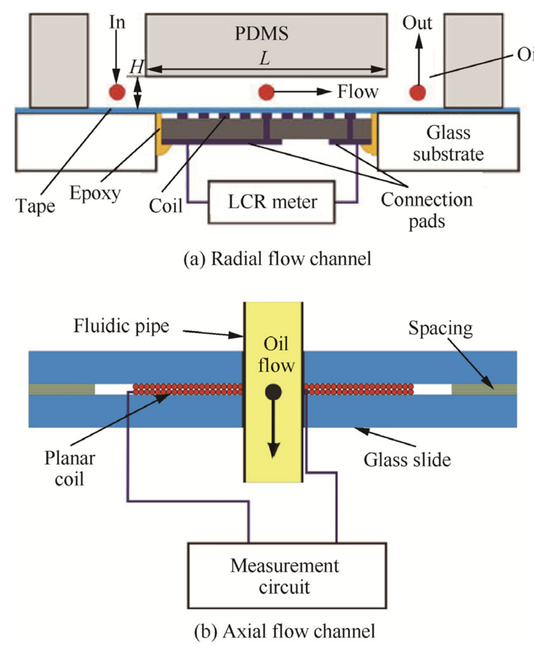

Fig. 13 Two debris sensor structures with high sensitivity.[81,82]

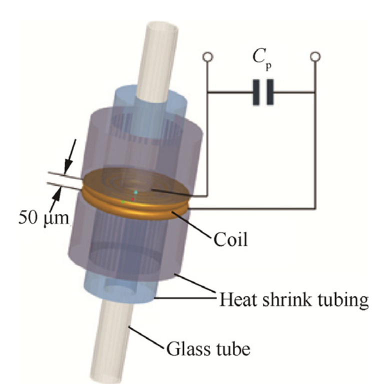

Fig. 14 LC resonance method to improve sensitivity.[85]

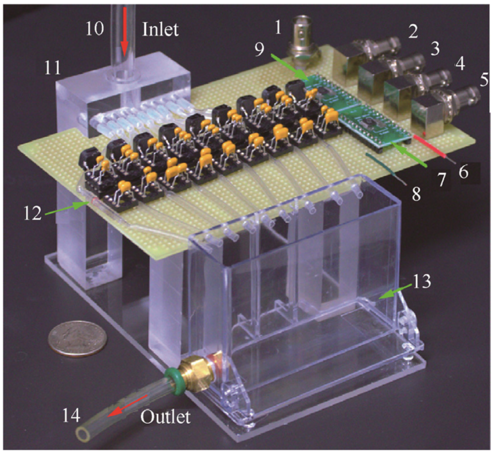

Fig. 15 Parallel sensing with multiple channels.[88]

netic debris can be detected in the previous pipe.[85] However, the flow capacity of this method is only 3 mL/min, which may not satisfy online debris detection. Therefore, Zhe's research group used parallel sensing in multiple channels to promote the flow capacity as shown in Fig. 15[83,88] (1. signal input/output, 2. control signal A1, 3. control signal A2, 4. control signal A3, 5. control signal A4, 6. multiplexer power inlet (DC, 13.0 V), 7. MUX2, 8. multiplexer channel enable voltage (DC, 3.6 V), 9. MUX1, 10. oil inlet, 11. flow divider, 12. sensing channel, 13. reservoir, and 14. oil outlet). In their latest study,[89] the flow capacity was improved to 460 mL/min through a 3 × 3 sensor array. In order to improve sensitivity in big flow conditions, Hong et al. analyzed axial and radial magnetic fields for debris detection, and found the radial field has a higher strength and uniformity than those of the axial field in the same excitation condition. Then, they presented a

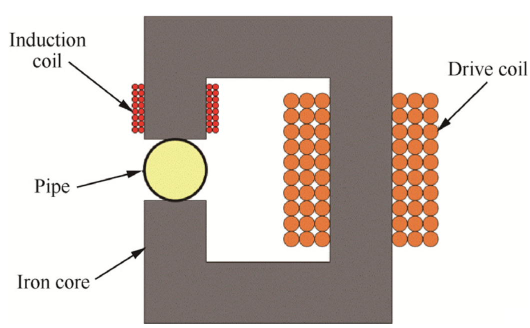

Fig. 16 Debris sensor based on a radial magnetic field.[86]

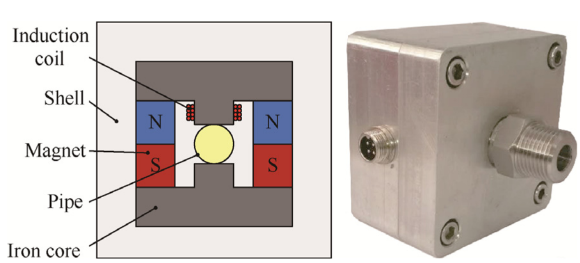

Fig. 17 A symmetrical structure with permanent magnets.[87]

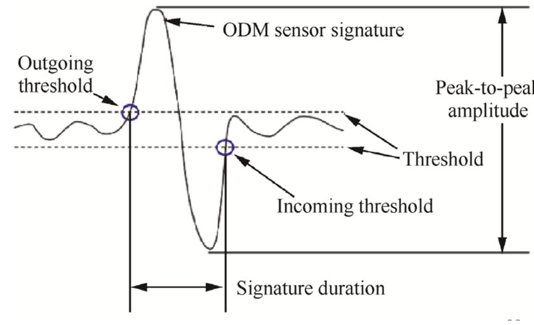

Fig. 18 Debris identification based on a threshold.[98]

sensor structure based on a radial magnetic field as shown in Fig. 16, which could detect 200 μm debris within a pipe with a diameter of 20 mm.[86] After that, they designed a symmetrical structure with permanent magnets to further optimize strength and uniformity, as shown in Fig. 17. Through this improvement, 83-μm debris could be detected within a pipe with a diameter of 12 mm under a flow rate of about 20 L/min,[87] which is valuable for practical applications.

As the sensitivity of practical detection is related to both sensor performance and environment interference, signal processing is another effective approach to improve sensitivity besides optimizing the structure and parameters.[83,98–102] Usually, debris signature is similar to a sine wave, and environment interference is composed by random noises and some periodical waveforms caused by mechanical vibration or AC power. Obviously, the sensor output combined with these waveforms is non-stationary, so a simple identification method for debris particles is threshold algorithm as shown in Fig. 18 (ODM: oil debris monitor), which is widely applied in practical detection.[9]

However, the performance of a threshold algorithm seriously depends on signal quality, i.e., smaller debris could be detected under a higher signal-to-noise ratio. Therefore, how to increase the signal-to-noise ratio is the key point. Hong and Liang presented an extraction method for debris signature based on the fractional calculus technique as shown in Fig. 19, of which the variables and algorithms are explained in Ref. [98] Fan et al.[99] considered that Kurtosis is a good indicator to distinguish non-periodical debris signature from stationary interference, so they presented a time-invariant wavelet transform combined with Kurtosis analysis as shown in Fig. 20 (TIWT: time-invariant wavelet transform, σ_j: standard deviation of the coefficients on the scale j, and N: length of sample data). In order to eliminate random noise and the interference caused by vibration, Bozchalooi and Liang[100] presented a joint method based on adaptive line enhancement and wavelet threshold de-noising as shown in Fig. 21 (ALE: adaptive line enhancement and IVE: iterative noise variance estimation). As the decomposition depth is an important parameter in the wavelet transform and directly affects the performance, Li et al. presented a maximal overlap discrete wavelet transform with an optimal decomposition depth as shown in Fig. 22, of which the detail is explained in Ref. [101] With a novel idea of de-noising, Hong et al.[102] presented a hybrid method combined with band pass filters and a correlation algorithm as shown in Fig. 23 ($x(t)$ is the data sampled from Sensor X, $y(t)$ is the data sampled from Sensor Y, and R_{xy} is the correlation result between $x(t)$ and $y(t)$), in which two signals come

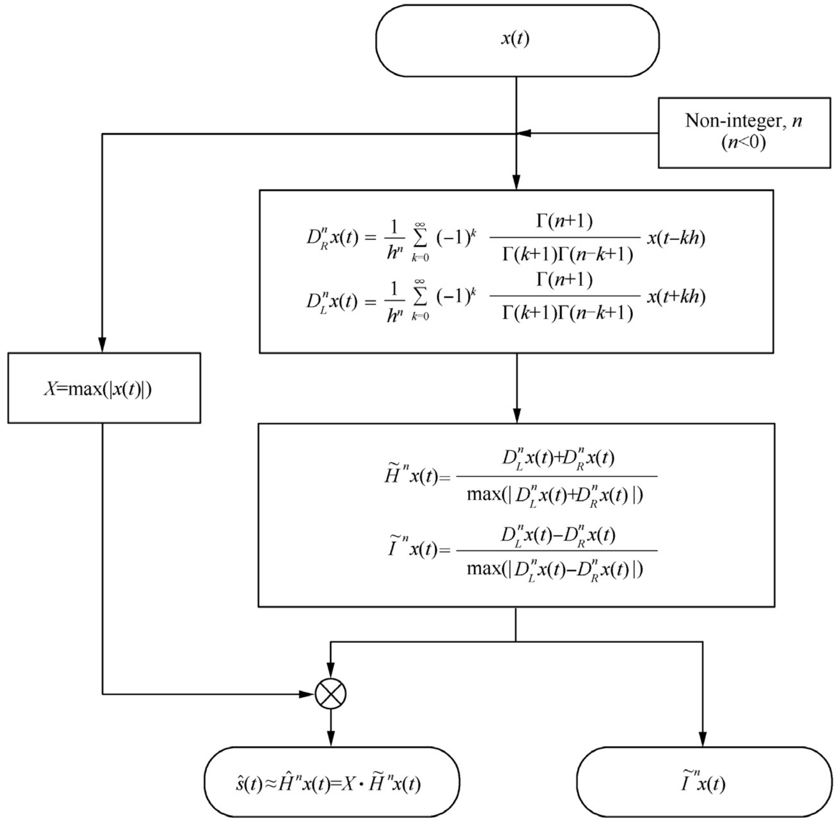

Fig. 19 Signal extraction method based on the fractional calculus technique.[98]

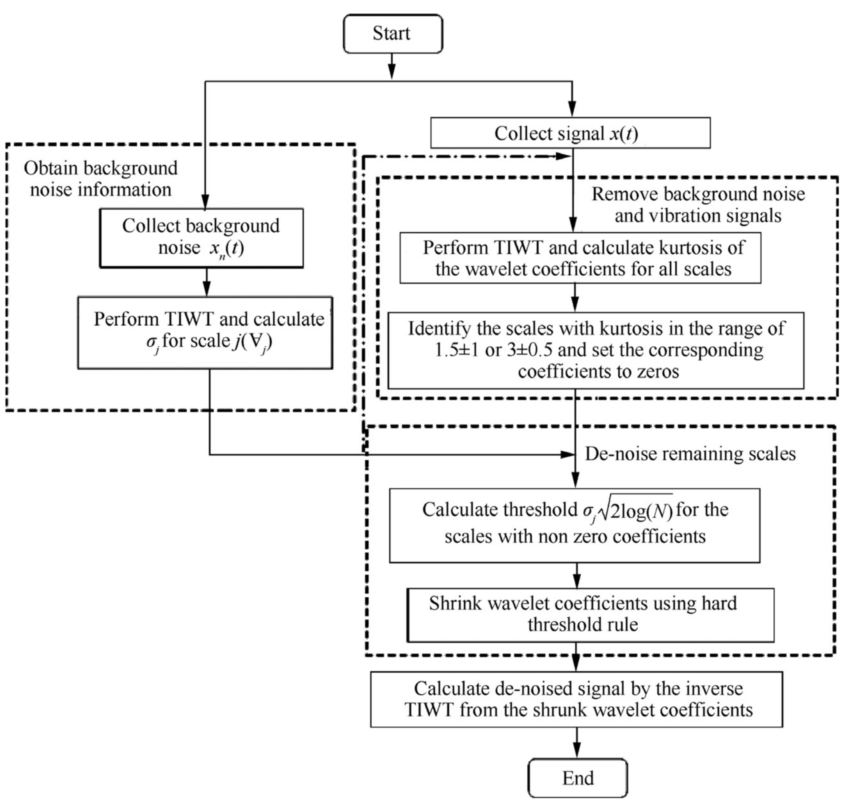

Fig. 20 A time-invariant wavelet transform combined with Kurtosis analysis.[99]

from two same sensors connected in series in a pipe. The experiment result indicated that this method can improve sensitivity to 2.63 times, i.e., the volume of minimum detectable debris is reduced to 38% of that from previous detection.

6. Debris-based diagnosis

In early 1970s, based on offline measuring oil samples or filters, engineers found that debris size and concentration were

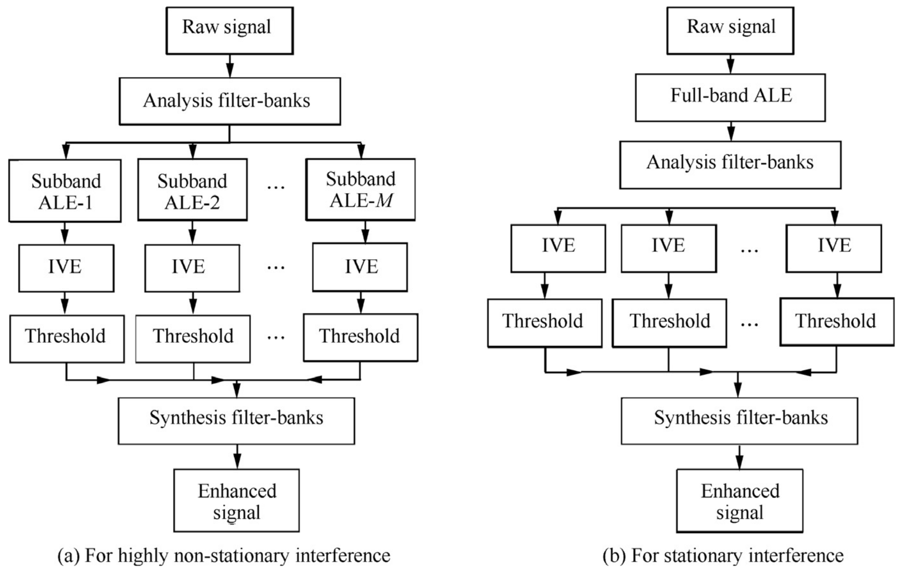

Fig. 21 A joint method based on adaptive line enhancement and wavelet threshold de-noising.[100]

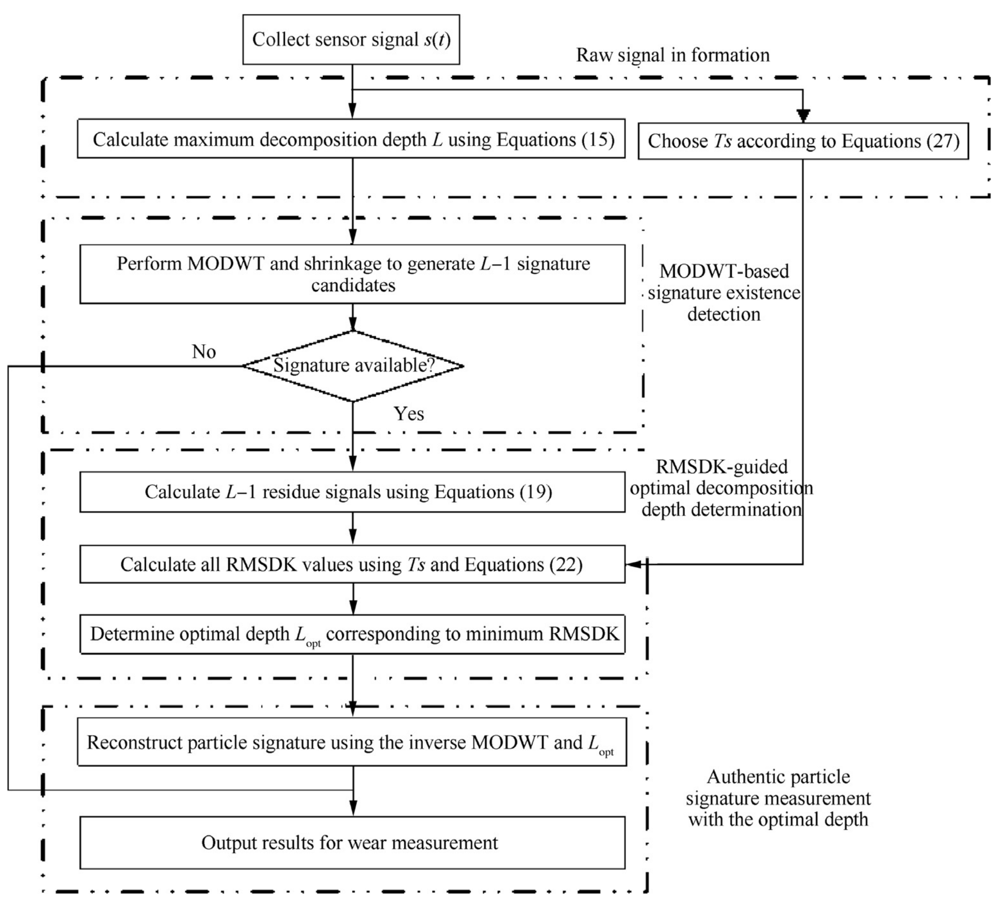

Fig. 22 A maximal overlap discrete wavelet transform with an optimal decomposition depth.[101]

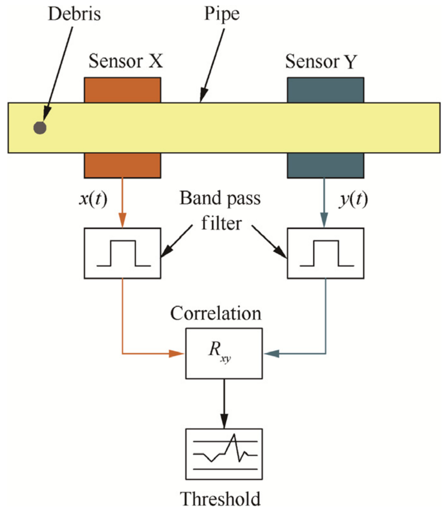

Fig. 23 A hybrid method combined with band pass filters and a correlation algorithm.[102]

apparently increased by increasing of wear severity.[6] Therefore, mechanical degradation could be known by regular debris inspections so that condition-based maintenance would be performed. Bowen and Anderson et al. studied debris sizes under different wear types, and found that debris size could roughly classify wear types and indicate wear severity, especially, above 15-μm debris particles generally coming from abnormal wear.[34,37] This study provided an important foundation for debris-based diagnosis. Further, Roylance and Pocock[39] analyzed 1–20 μm debris in different wear situations, and proposed Weibull function to describe the debris distribution so that the wear progress can be revealed through the distribution parameter. As research continued, many studies[3,7,68,69] indicated that the relationships between wear type, wear mechanism, and debris feature are complicated. In practical wear, several wear mechanisms may occur at the same time, and several debris types would be generated. Therefore, it is difficult to know current wear progress through classifying current debris, i.e., the debris classification result may not determine whether a machine is normal or not.

By contrast, online debris detection not only provides debris size and number at a moment, but also shows their dynamic processes.[8,76,77] This advantage can increase confidence in diagnosing by specified criteria. In 1980s, Centers and Price[8] compared a quantitative debris monitor (QDM) to offline debris detection as shown in Fig. 24, which indicated that the sensor can monitor debris generation through accumulated debris counts. In 2000, Miller and Kitaljevich[9] investigated the bearing fault of an F119 engine by using a MetalSCAN sensor and achieved fault alarm through setting a limit of accumulated debris counts, as shown in Fig. 25. After that, Dempsey used a MetalSCAN sensor to monitor the wear processes of gears[103] and bearings[104] respectively shown in Figs. 26 and 27. The experiment results indicated that the accumulated debris mass can also reflect the wear progress. As debris sizes are variable, the accumulated mass is more real than accumulated counts to measure friction damage. Nevertheless, further studies[10,104] indicated that it is still difficult to determine a threshold of the accumulated mass to distinguish fault components from

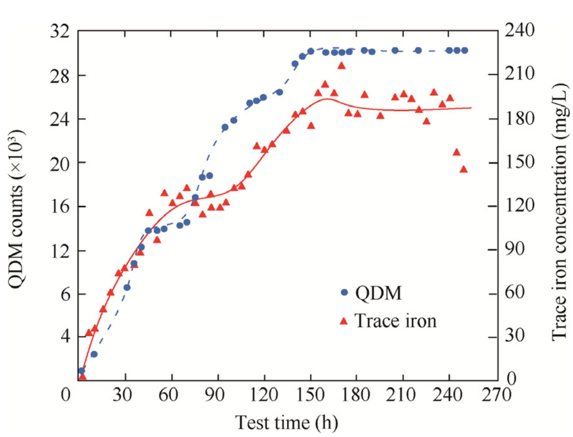

Fig. 24 Quantitative debris monitor vs offline debris detection.[8]

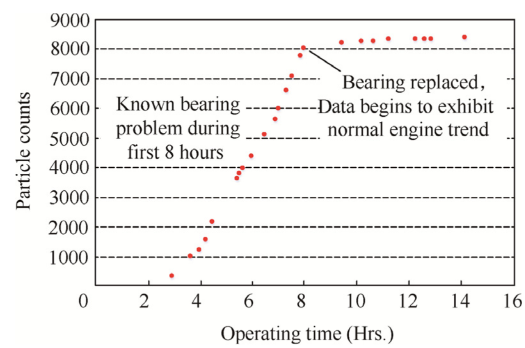

Fig. 25 Debris monitoring for an F119's bearing based on a MetalSCAN sensor.[9]

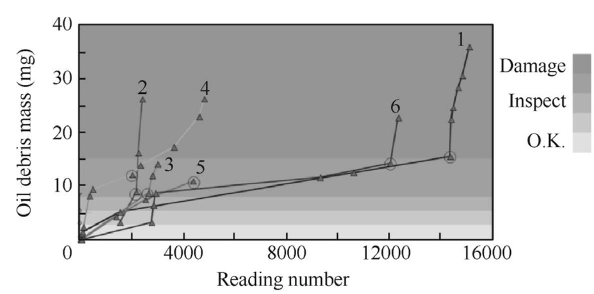

Fig. 26 Debris monitoring for gears based on a MetalSCAN sensor[103]

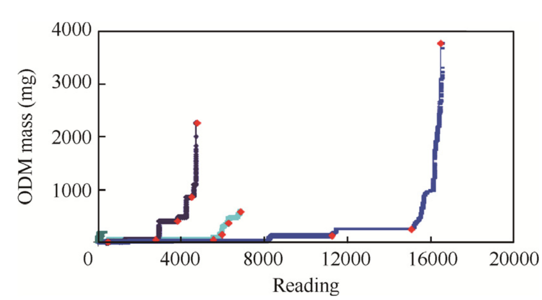

Fig. 27 Debris monitoring for bearings based on a MetalSCAN sensor[104]

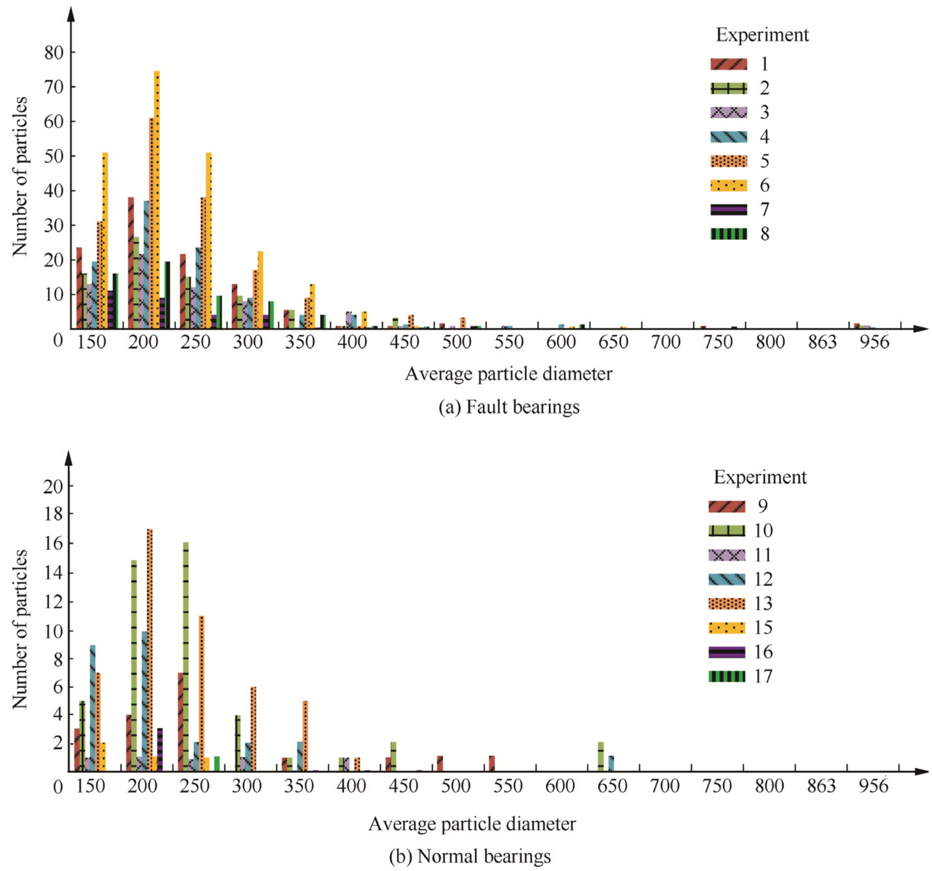

Fig. 28 Debris distribution comparison.[25]

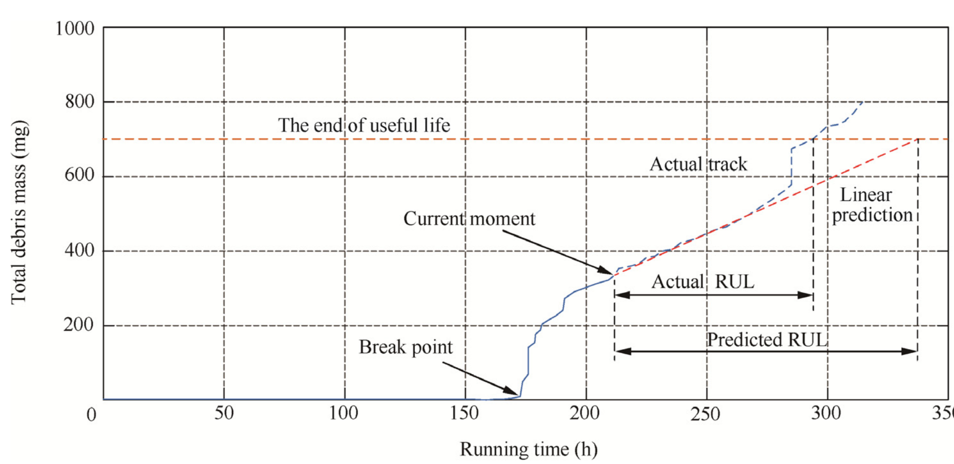

Fig. 29 A simple linear model to predict the remaining useful life (RUL).

normal ones because of an inconsistent initial state and a variable running condition, even their distributions are very similar as shown in Fig. 28. In addition, the underlying reason is the cumulant of debris is little related to the physical running status.

As debris generation is irreversible, the remaining useful life predicted through debris information has a good convergence. A typical debris generation behavior commonly exists in the degradation of gears and bearings[9,10,25,103–105]: a few debris particles are generated in the early and middle stages of a component's useful life, and the generation rate will rapidly increase and tend to be a stable value in the late stage. Therefore, the remaining useful life can be roughly predicted by a simple linear model when an accumulated debris amount is defined as the end of useful life,[10] as shown in Fig. 29. However, in a complicated machine such as a wind turbine, there are many friction pairs, and their working loads may frequently change in a large range so that the debris generation rate is variable; as a result, a simple linear model is no longer applicable. Thus, Dupuis presented a model with combined

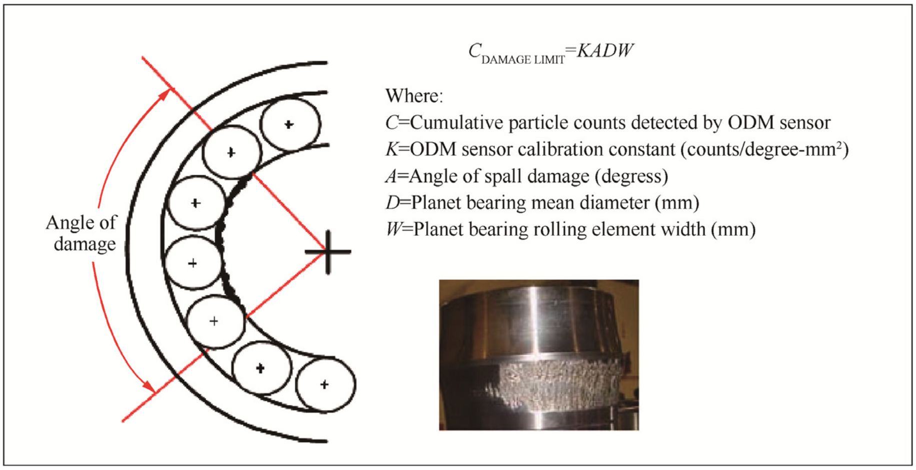

Fig. 30 Definition of the damage limit.[11]

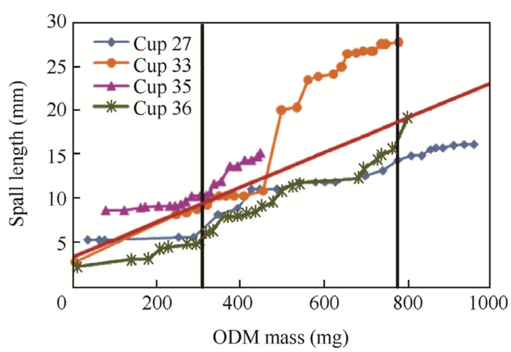

Fig. 31 Definitions of the maximum and minimum damage levels.[10]

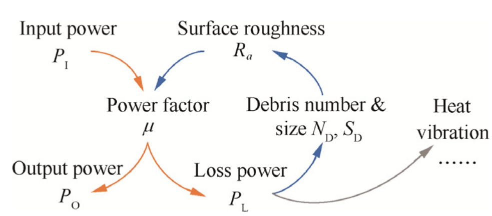

Fig. 32 Positive feedback model for debris generation.[106]

average generation rates of both long term and short term to predict the remaining useful life of a wind turbine.[11] The model is shown in Eqs. (2)–(4), where MA_S is the short-term moving average, MA_L is the long-term moving average, MA_W is the weighted moving average, C is the daily accumulated count, and n is the current day. L is the number of days of long term while S is the number of days of short term. For the definition of damage limit, the total mass of the expected damage area is usually defined as the end of useful life as shown in Fig. 30. Nevertheless, Dempsey et al. found that the ratio of total mass to damage area is variable, so they considered a compromise to define the maximum and minimum damage levels for the remaining useful life,[10] as shown in Fig. 31, where cups 27, 33, 35, and 36 are four bearing cups among experimental samples. In order to explain the sudden change of the debris generation rate, Hong et al.[106] presented a positive feedback mechanism to describe the behavior of debris generation as shown in Fig. 32, and they proposed a certain level of sudden change of the generation rate as the end of useful life. Based on this idea, they developed a prediction model for remaining useful life as shown in Eq. (5), where η is the remaining useful life, ξ_R is the working condition factor, R_{a0} is the initial surface roughness, and t is the running time. The predicted result for a wind turbine indicated that the remaining useful life can be effectively predicted in the early and middle stages of the whole life, as shown in Fig. 33, where MAM is the moving average model, PFM is the positive feedback model, and FLD is the full life data. This study differs from traditional debris classification to reveal wear behavior and is a new trial form time series of debris generation.

$$MA_S = \left(C_n + C_{n-1} + \ldots + C_{n-(S-1)}\right)/S \tag{2}$$

$$MA_L = \left(C_n + C_{n-1} + \ldots + C_{n-(L-1)}\right)/L \tag{3}$$

$$MA_W = MA_L + MA_S \tag{4}$$

$$\eta = \frac{1}{\xi_R R_{a0}^2} - t \tag{5}$$

7. Discussion

This paper has summarized research progresses on mechanical wear debris related fields such as wear mechanisms, debris features, detection methods, signal processing, and fault diagnosis. The following conclusions can be obtained. Because of its close relationship with friction wear, wear debris provides powerful information for mechanical diagnosis. The related studies indicate that wear mechanisms and types can be roughly identified through debris features, but debris classification may not be able to determine the wear progress because several wear mechanisms may simultaneously exist in a practical wearing process. With the maturity of online inductive debris sensors, online debris monitoring becomes popular and shows excellent performance on mechanical wear tracking. As new indicators, accumulated debris mass and number can effectively alarm mechanical fault and predict remaining useful life. However, the accumulation may not reflect the current

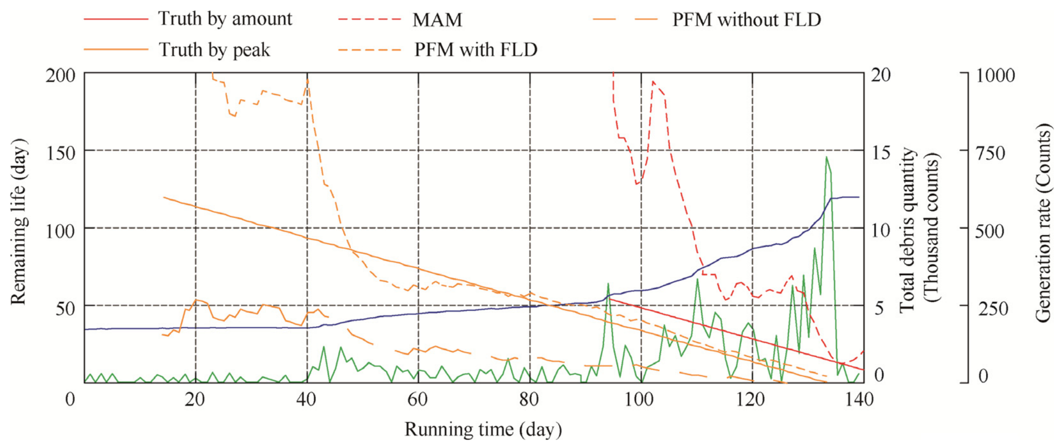

Fig. 33 Predicted results of the moving average model and the positive feedback model.[106]

wear status, so diagnosis results based on these indicators would be seriously affected by individual varieties. In order to promote wider applications of debris techniques, the authors feel that the following issues are worth further studies.

(1) As existing debris features such as size and distribution are difficult to determine wear progress, debris features with time attributes, e.g., debris accumulation and generation rate, should be further investigated to reveal wear behavior.
(2) Debris information obtained from current online detection is limited to size, number, and material type, so enhancing online detection by including debris morphology and composition will contribute to online fault diagnosis.
(3) Compared to offline debris detection methods, online debris monitoring can provide a detailed process of debris generation rather than rich information of each debris particle. Therefore, how to reveal wear modes based on debris generation behaviors would be a significant study.
(4) There may exist several friction surfaces in a single machine, but with only one lubrication system, debris generated from different friction surfaces will be mixed together, and abnormal wear might be hidden, causing a severe catastrophe to the machine. Therefore, how to distinguish different debris sources and track wear processes would also be an interesting topic.

Acknowledgements

This study was supported by the National Natural Science Foundation of China (Nos. 51620105010 and 51575019), the National Basic Research Program of China (No. 2014CB046402), and Singapore Energy Innovation Research Programme (Gas Technology Grant No. NRF2014EWT-EIRP003-014).

References

1. Jardine AKS, Lin D, Banjevic D. A review on machinery diagnostics and prognostics implementing condition-based maintenance. *Mech Syst Signal Process* 2006;**20**(7):1483–510.
2. Amiri M, Khonsari MM. On the thermodynamics of friction and wear – a review. *Entropy* 2010;**12**(5):1021.
3. Dwyer-Joyce R, Williams JA, Roylance BJ. Wear debris and associated wear phenomena—fundamental research and practice. *Pro Inst Mech Eng, Part J: J Eng Tribol* 2000;**214**(1):79–105.
4. Dowson D. *History of tribology*. 2nd ed. New Jersey: Wiley; 1998.
5. Fouvry S, Liskiewicz T, Kapsa P, Hannel S, Sauger E. An energy description of wear mechanisms and its applications to oscillating sliding contacts. *Wear* 2003;**255**(1–6):287–98.
6. Scott D. Debris examination—a prognostic approach to failure prevention. *Wear* 1975;**34**(1):15–22.
7. Roylance BJ. Ferrography—then and now. *Tribol Int* 2005;**38**(10):857–62.
8. Centers PW, Price FD. Real time simultaneous in-line wear and lubricant condition monitoring. *Wear* 1988;**123**(3):303–12.
9. Miller JL, Kitaljevich D. In-line oil debris monitor for aircraft engine condition assessment. 2000 March 25-25; Big Sky, MT, USA, USA. Piscataway,NJ: IEEE Press; 2002. p. 49-56.
10. Dempsey PJ, Bolander N, Haynes C, Toms AM. Investigation of bearing fatigue damage life prediction using oil debris monitoring. National Aeronautics and Space Administration: Glenn Research Center; 2011. Report No.: NASA/TM-2011-217117, E-17804.
11. Dupuis R. Application of oil debris monitoring for wind turbine gearbox prognostics and health management. *Annual conference of the prognostics and health management society*; 2010 October 13–16th; Portland, Oregon, USA. p. 10–6.
12. Williams JA. Wear and wear particles—some fundamentals. *Tribol Int* 2005;**38**(10):863–70.
13. Richardson R. The wear of metals by hard abrasives. *Wear* 1967;**10**(4):291–309.
14. Archard J. Contact and rubbing of flat surfaces. *J Appl Phys* 1953;**24**(8):981–8.
15. Archard J, Hirst W. The wear of metals under unlubricated conditions. *Proc Roy Soc Lond A: Math, Phys Eng Sci* 1956;**236**(1206):397–410.
16. Rabinowicz E, Tanner RI. Friction and wear of materials. *J Appl Mech* 1966;**33**(2):479–86.
17. Muro H, Tsushima T, Nagafuchi M. Initiation and propagation of surface cracks in rolling fatigue of high hardness steel. *Wear* 1975;**35**(2):261–82.
18. Yamamoto T. Crack growth in lubricated rollers. *Solid Contact and Lubrication* 1980;**39**:223–36.
19. Leng X, Chen Q, Shao E. Initiation and propagation of case crushing cracks in rolling contact fatigue. *Wear* 1988;**122**(1):33–43.
20. Olver AV. The mechanism of rolling contact fatigue: an update. *Proc Inst Mech Eng, Part J: Eng Tribol* 2005;**219**(5):313–30.

21. Webster M, Norbart C. An experimental investigation of micropitting using a roller disk machine. *Tribol Trans* 1995;**38**(4):883–93.
22. Shotter B. Micropitting: its characteristics and implications on the test requirements of gear oils. *Perform Test Gear Oils Trans Fluids, Inst Petrol* 1981;53–60.
23. Sayles R, Macpherson P. Influence of wear debris on rolling contact fatigue. *ASTM Int* 1982;**771**:255–74.
24. Lorösch H-K. Research on longer life for rolling-element bearings. *Lubr Eng* 1985;**41**(1):37–43.
25. Dempsey PJ, Lewicki DG, Decker HJ. Investigation of gear and bearing fatigue damage using debris particle distributions. DTIC Document. Report No.: NASA-GRC-E-14297; 2004.
26. Burwell J, Strang C. On the empirical law of adhesive wear. *J Appl Phys* 1952;**23**(1):18–28.
27. Odi-Owei S, Roylance B, Xie L. An experimental study of initial scuffing and recovery in sliding wear using a four-ball machine. *Wear* 1987;**117**(3):267–87.
28. Kwon OK. A study of the interaction of chemical, thermal and mechanical factors in a lubricated sliding contact: thermally-activated wear theory [dissertation]. Swansea: University College of Swansea; 1981.
29. Rabinowicz E. An adhesive wear model based on variations in strength values. *Wear* 1980;**63**(1):175–81.
30. Blau PJ. Mechanisms for transitional friction and wear behavior of sliding metals. *Wear* 1981;**72**(1):55–66.
31. Seifert WW, Westcott VC. A method for the study of wear particles in lubricating oil. *Wear* 1972;**21**(1):27–42.
32. Yarrow A, Gadd P. The role of ferrography in the monitoring of helicopter assemblies. *Proceedings of the international conference on condition monitoring*. 1984 April; University of Swansea; 1984. p. 503–24.
33. Dowson D, Dalmaz G, Childs T, Taylor C, Godet M. *Wear particles: from the cradle to the grave*. Amsterdam: Elsevier; 1992.
34. Anderson DP. Wear particle atlas. Lakehurst (NJ): Naval Air Engineering Center, Department SEE; 1982. Report No.: NAEC-92-165.
35. Roylance B, Raadnui S. The morphological attributes of wear particles—their role in identifying wear mechanisms. *Wear* 1994;**175**(1):115–21.
36. Eisentraut KJ, Newman RW, Saba CS, Kauffman RE, Rhine WE. Spectrometric oil analysis. Detecting engine failures before they occur. *Anal Chem* 1984;**56**(9):1086A–94A.
37. Bowen ER, Westcott VC. Wear particle atlas. Burlington: Foxboro/Trans-Sonics, Inc. Report No.: N00156-74-C-1682; 1976.
38. Fitch B. Anatomy of wear debris. *Mach Lubr* 2013(10).
39. Roylance B, Pocock G. Wear studies through particle size distribution I: application of the Weibull distribution to ferrography. *Wear* 1983;**90**(1):113–36.
40. Roylance B. Monitoring gear wear using debris analysis—prospects for establishing a prognostic method. *Proceedings of the 5th international congress on tribology*, 1989 June 12; Espoo, Finland. Espoo: Finnish Society for Tribology; 1989. p. 85.
41. Raadnui S, Roylance BJ. The classification of wear particle shape. *Lubr Eng* 1995;**51**(5):432–7.
42. Peng Z, Kirk T, Xu Z. The development of three-dimensional imaging techniques of wear particle analysis. *Wear* 1997;**203**:418–24.
43. Peng Z, Kirk T. Computer image analysis of wear particles in three-dimensions for machine condition monitoring. *Wear* 1998;**223**(1):157–66.
44. Yeung KK, McKenzie AJ, Liew D, Luoma GA. Development of computer-aided image analysis for filter debris analysis. *Lubr Eng* 1994;**50**(4):293–9.
45. Myshkin N, Kong H, Grigoriev AY, Yoon E-S. The use of color in wear debris analysis. *Wear* 2001;**251**(1):1218–26.
46. Finkin EF. The wear of copper, aluminum, mild steel, and zinc, and their wear particle shape factors. *ASLE Trans* 1964;**7**(4):377–82.
47. Roylance BJ, Albidewi I, Laghari M. Computer-aided vision engineering (CAVE)-quantification of wear particle morphology. *Lubr Eng* 1994;**50**(2).
48. Beddow JK, Fong S-T, Vetter A. Morphological analysis of metallic wear debris. *Wear* 1980;**58**(2):201–11.
49. Thomas A, Davies T, Luxmoore A. Computer image analysis for identification of wear particles. *Wear* 1991;**142**(2):213–26.
50. Kirk T, Stachowiak G. Development of fractal morphological descriptors for a computer Image analysis system. *Proceedings of international tribology conference*. 1990 December 2–5; Barton, Australia. Barton, ACT: Institution of Engineers; 1990.
51. Kirk T, Stachowiak G, Batchelor A. Fractal parameters and computer image analysis applied to wear particles isolated by ferrography. *Wear* 1991;**145**(2):347–65.
52. Stachowiak G, Kirk T, Stachowiak G. Ferrography and fractal analysis of contamination particles in unused lubricating oils. *Tribol Int* 1991;**24**(6):329–34.
53. Podsiadlo P, Kuster M, Stachowiak G. Numerical analysis of wear particles from non-arthritic and osteoarthritic human knee joints. *Wear* 1997;**210**(1):318–25.
54. Zhang MQ, Lu ZP, Friedrich K. On the wear debris of polyetheretherketone: fractal dimensions in relation to wear mechanisms. *Tribol Int* 1997;**30**(2):87–102.
55. Podsiadlo P, Stachowiak G. Evaluation of boundary fractal methods for the characterization of wear particles. *Wear* 1998;**217**(1):24–34.
56. Stachowiak G. Numerical characterization of wear particles morphology and angularity of particles and surfaces. *Tribol Int* 1998;**31**(1):139–57.
57. Shirong G, Guoan C, Xiaoyun Z. Fractal characterization of wear particle accumulation in the wear process. *Wear* 2001;**251**(1):1227–33.
58. Yuan C, Li J, Yan X, Peng Z. The use of the fractal description to characterize engineering surfaces and wear particles. *Wear* 2003;**255**(1):315–26.
59. Hamblin M, Stachowiak G. Characterisation of surface abrasivity and its relation to two-body abrasive wear. *Wear* 1997;**206**(1):69–75.
60. Podsiadlo P, Stachowiak G. 3-D imaging of surface topography of wear particles found in synovial joints. *Wear* 1999;**230**(2):184–93.
61. Stachowiak G, Podsiadlo P. Surface characterization of wear particles. *Wear* 1999;**225**:1171–85.
62. Podsiadlo P, Stachowiak G. Scale-invariant analysis of wear particle morphology—a preliminary study. *Tribol Int* 2000;**33**(3):289–95.
63. Podsiadlo P, Stachowiak G. Scale-invariant analysis of wear particle surface morphology: I. Theoretical background, computer implementation and technique testing. *Wear* 2000;**242**(1):160–79.
64. Peng Z, Kirk T. Wear particle classification in a fuzzy grey system. *Wear* 1999;**225**:1238–47.
65. Peng Z, Kirk T. Two-dimensional fast Fourier transform and power spectrum for wear particle analysis. *Tribol Int* 1997;**30**(8):583–90.
66. Podsiadlo P, Stachowiak G. Scale-invariant analysis of wear particle surface morphology: II. Fractal dimension. *Wear* 2000;**242**(1):180–8.
67. Podsiadlo P, Stachowiak G. Scale-invariant analysis of wear particle surface morphology: III. Pattern recognition. *Wear* 2000;**242**(1):189–201.
68. Raadnui S. Wear particle analysis—utilization of quantitative computer image analysis: a review. *Tribol Int* 2005;**38**(10):871–8.
69. Bhushan B. *Modern tribology handbook*. CRC Press; 2000.

70. Burrows JA, Heerdt J, Willis J. Determination of wear metals in used lubricating oils by atomic absorption spectrometry. *Anal Chem* 1965;**37**(4):579–82.
71. Whitlock RR, Humprey GR, Churchill DB. The path to affordable long term failure warning: the XRF-wear monitor. Washington, D.C.: Naval Research Lab 1998. Report No.: AD-A348000.
72. Toms AM, Cassidy K. Filter debris analysis for aircraft engine and gearbox health management. *J Fail Anal Prev* 2008;**8**(2):183–7.
73. Kayani S. Using combined XRD-XRF analysis to identify meteorite ablation debris. 2009 October 19–20; Islamabad, Pakistan. Piscataway, NJ: IEEE Press; 2017.p. 219–20.
74. Chambers KW, Arneson MC, Waggoner CA. An on-line ferromagnetic wear debris sensor for machinery condition monitoring and failure detection. *Wear* 1988;**128**(3):325–37.
75. Zhu X, Zhong C, Zhe J. Lubricating oil conditioning sensors for online machine health monitoring – a review. *Tribol Int* 2017;**109**:473–84.
76. Yan L, Wen SZ, Xie YB, Zhao F. Advances in research on a multi-channel on-line ferrograph. *Tribol Int* 1997;**30**(4):279–82.
77. Tucker J, Reintjes J, Duncan M, McClelland T, Tankersley L. Lasernet fines optical oil debris monitor. Washington, D.C.: Naval Research Lab Section L; 1998. Report No.: ADA347453.
78. Rheims J, Wriedt T, Bauckhage K. Sizing of inhomogeneous particles by a differential laser Doppler anemometer. *Meas Sci Technol* 1999;**10**(2):68.
79. Wu T, Wu H, Du Y, Kwok N, Peng Z. Imaged wear debris separation for on-line monitoring using gray level and integrated morphological features. *Wear* 2014;**316**(1–2):19–29.
80. Flanagan IM, Jordan JR, Whittington HW. An inductive method for estimating the composition and size of metal particles. *Meas Sci Technol* 1990;**1**(5):381.
81. Du L, Zhe J, Carletta J, Veillette R, Choy F. Real-time monitoring of wear debris in lubrication oil using a microfluidic inductive Coulter counting device. *Microfluid Nanofluid* 2010;**9**(6):1241–5.
82. Du L, Zhe J. A high throughput inductive pulse sensor for online oil debris monitoring. *Tribol Int* 2011;**44**(2):175–9.
83. Du L, Zhe J. Parallel sensing of metallic wear debris in lubricants using undersampling data processing. *Tribol Int* 2012;**53**:28–34.
84. Du L, Zhe J. An integrated ultrasonic–inductive pulse sensor for wear debris detection. *Smart Mater Struct* 2013;**22**(2):025003.
85. Du L, Zhu X, Han Y, Zhao L, Zhe J. Improving sensitivity of an inductive pulse sensor for detection of metallic wear debris in lubricants using parallel LC resonance method. *Meas Sci Technol* 2013;**24**(7):075106.
86. Hong W, Wang S, Tomovic M, Han L, Shi J. Radial inductive debris detection sensor and performance analysis. *Meas Sci Technol* 2013;**24**(12):125103.
87. Hong W, Wang S, Tomovic MM, Liu H, Wang X. A new debris sensor based on dual excitation sources for online debris monitoring. *Meas Sci Technol* 2015;**26**(9):095101.
88. Zhu X, Du L, Zhe J. An integrated lubricant oil conditioning sensor using signal multiplexing. *J Micromech Microeng* 2015;**25**(1):015006.
89. Zhu X, Du L, Zhe J. A 3×3 wear debris sensor array for real time lubricant oil conditioning monitoring using synchronized sampling. *Mech Syst Signal Process* 2017;**83**:296–304.
90. Megerle CA, inventor; Hughes Aircraft Company, assignee. Oil quality monitor sensor and system. United States patent US5089780 A, 1992 February 18.
91. Mauntz MR, Gegner J, Kuipers U, Klingau S. A sensor system for online oil condition monitoring of operating components. In: Gegner J, editor. *Tribology—Fundamentals and Advancement*; 2013.p. 305–21.
92. Zhe J, Choy F, Murali S, Sarangi M, Wilfong R. Oil debris detection using capacitance and ultrasonic measurements. *Proceedings of ASME/STLE 2007 international joint tribology conference*. 2007 October 22–24, American Society of Mechanical Engineers, San Diego, California, USA; 2007. p. 113–5.
93. Murali S, Jagtiani AV, Xia X, Carletta J, Zhe J. A microfluidic Coulter counting device for metal wear detection in lubrication oil. *Rev Sci Instrum* 2009;**80**(1):016105.
94. Murali S, Xia X, Jagtiani AV, Carletta J, Zhe J. Capacitive Coulter counting: detection of metal wear particles in lubricant using a microfluidic device. *Smart Mater Struct* 2009;**18**(3):037001.
95. Wen Z, Yin X, Jiang Z. Applications of electrostatic sensor for wear debris detecting in the lubricating oil. *J Inst Eng (India): Series C* 2013;**94**(3):281–6.
96. Nemarich CP, Whitesel HK, Sarkady A. On-line wear particle monitoring based on ultrasonic detection and discrimination. David Taylor Research Center; 1988. Report No.: ADA212956.
97. Xu C, Zhang P, Wang H, Li Y, Lv C. Ultrasonic echo waveshape features extraction based on QPSO-matching pursuit for online wear debris discrimination. *Mech Syst Signal Process* 2015;**60–61**:301–15.
98. Hong H, Liang M. A fractional calculus technique for on-line detection of oil debris. *Meas Sci Technol* 2008;**19**(5):055703.
99. Fan X, Liang M, Yeap T. A joint time-invariant wavelet transform and kurtosis approach to the improvement of in-line oil debris sensor capability. *Smart Mater Struct* 2009;**18**(8):085010.
100. Bozchalooi IS, Liang M. In-line identification of oil debris signals: an adaptive subband filtering approach. *Meas Sci Technol* 2010;**21**(1):015104.
101. Li C, Peng J, Liang M. Enhancement of the wear particle monitoring capability of oil debris sensors using a maximal overlap discrete wavelet transform with optimal decomposition depth. *Sensors (Basel)* 2014;**14**(4):6207–28.
102. Hong W, Wang S, Liu H, Tomovic MM, Chao Z. A hybrid method based on band pass filter and correlation algorithm to improve debris sensor capacity. *Mech Syst Signal Process* 2017;**82**:1–12.
103. Dempsey PJ. Gear damage detection using oil debris analysis. NASA Glenn Research Center; 2001. Report No.: NASA/TM-2001-210936.
104. Dempsey PJ, Kreider G, Fichter T. Investigation of tapered roller bearing damage detection using oil debris analysis. *Proceedings of 2006 IEEE aerospace conference*. 2006 March 4–11; Big Sky, USA. Piscataway, NJ: IEEE Press; 2006.
105. Dempsey PJ, Afjeh AA. Integrating oil debris and vibration gear damage detection technologies using fuzzy logic. *J Am Helicopter Soc* 2004;**49**(2):109–16.
106. Hong W, Wang S, Tomovic MM, Liu H, Shi J, Wang X. A novel indicator for mechanical failure and life prediction based on debris monitoring. *IEEE Trans Reliab* 2016;**66**(1):161–9.